FREEZE-FRACTURE IDENTIFICATION OF STEROL-DIGITONIN COMPLEXES IN CELL AND LIPOSOME MEMBRANES

PETER M. ELIAS, JON GOERKE, and DANIEL S. FRIEND, with the technical assistance of BARBARA E. BROWN

From the Departments of Dermatology, Physiology, and Pathology, and the Cardiovascular Research Institute, University of California School of Medicine, San Francisco, California 94143, and the Dermatology Section, Veterans Administration Hospital, San Francisco, California 94121

ABSTRACT

To advance our understanding of the organization of cholesterol within cell membranes, we used digitonin in freeze-fracture investigations of model lipid vesicles and tissues. Cholesterol suspensions or multilamellar liposomes composed of phosphatidylcholine with and without cholesterol were exposed to digitonin. Freeze-fracture replicas of those multilamellar liposomes containing cholesterol displayed either 50–60-nm wide intramembrane corrugations or extramembrane tubular complexes. Comparable intramembrane hemitubular scallops and extracellular free tubular complexes were observed in thin sections. Exposure of sperm, erythrocytes (whole and ghosts), and intact tissues (skin, liver, adrenal gland, epididymis) to digitonin produced the same types of intra- and extramembrane complexes or furrows as were formed in liposomes. The plasma membrane of guinea pig serum tail had two unfurrowed regions: the annulus and the zipper. Incubating erythrocyte membranes with digitonin resulted in rapid displacement of cholesterol, accompanied by intramembrane particle clustering and membrane faceting, a feature which we did not see in the intact epithelia studied. In freeze-fractured epithelia, we found that plasma membranes, lysosomes, and some vesicular organelles commonly furrowed, but that mitochondrial membranes and nuclear envelopes were generally spared, correlating well with their known cholesterol content. Finally, plasma membrane corrugations approached but did not impinge on either gap or tight junctions, or on coated vesicles.

We conclude that freeze-fracture of membranes exposed to digitonin: (*a*) reveals distinctive cholesterol-digitonin structural complexes; (*b*) distinguishes cholesterol-rich and -poor organelle membranes; and (*c*) demonstrates membrane domains rich or poor in cholesterol.

KEY WORDS freeze-fracture · cytochemistry · cholesterol · liposomes · membranes

Phospholipids, proteins, and carbohydrates are thought to be inhomogeneously distributed within the membrane bilayer (reviewed in references 4, 32, 41, 48, 52), but little is yet known about cholesterol in this regard ([20] reviewed in references 7, 31, 43). Although cholesterol is present in cell membranes, cell fractionation studies have

revealed wide variations in the cholesterol concentration of different organelles (reviewed in references 11, 31). For example, most plasma membranes and the membranes of Golgi complex, lysosomes, and smooth microsomes are sterol-rich compared with the membranes of mitochondria, nuclear envelope, and rough endoplasmic reticulum. In addition, there also may be regional variations in cholesterol content within individual membranes (41). For example, the boundary region around some integral membrane proteins is said to be sterol-free (57), and the lipid composition of gap junctions (26) and coated vesicles (44) has been found to differ from that of whole plasma membranes. Finally, membrane lipid composition, again including cholesterol, differs in various pathological and physiological states (10, 15, 31, 49).

A technique capable of identifying cholesterol-rich regions within biological membranes would offer a new means of studying membrane composition and supramolecular organization (30). The glycosylated sterol digitonin is well suited for this purpose. It combines with unesterified 3-β-hydroxysterols (predominantly free cholesterol in animal tissues), and produces precipitates that are relatively insoluble in organic solvents (5, 12, 50, 60). As a result, many of the sterol-digitonin complexes remain in situ during routine processing through solvents for thin-section electron microscopy (1, 39, 40, 46, 47, 53), and produce plasma membrane scallops or extracellular tubular complexes (24, 25, 27, 36, 42, 59). In this paper, we describe a method for using digitonin for freeze-fracture preparations, relate morphological features to quantitative biochemical data on sterol retention, and demonstrate the application of this method to the study of membrane heterogeneity in tissues and in isolated cells. To delineate further the characteristics, requirements, and optimal conditions for the use of digitonin, we also applied the technique to lipid vesicles. With this model system, we then investigated the effects of fixation, temperature, and the presence of other lipids on the formation of sterol-digitonide complexes. Portions of this work have appeared in abstract form (19).

MATERIALS AND METHODS

Tissue Sources

We examined dermis, epidermis, adrenal gland, and liver from Swiss albino mice; epididymis and suspensions of sperm from guinea pigs; and human erythrocytes and erythrocyte ghosts. The ghosts were freshly prepared by the method of Dodge et al. (13) before application of digitonin.

Digitonin Exposure

LIPOSOMES: Multilamellar liposomes were prepared by combining egg phosphatidylcholine (Sigma Chemical Co., St. Louis, Mo.), decolorized by passage over charcoal in methanol, with 4× recrystallized cholesterol (ICN Pharmaceuticals, Inc., Cleveland, Ohio) at 1:1, 2:1, and 5:1 mole ratios. Single component phosphatidylcholine liposomes and cholesterol suspensions were also prepared. ~10 mg of each lipid or lipid mixture was dissolved in chloroform and evaporated to dryness as a film on a round-bottom flask. Liposomes were formed by gently resuspending the lipids, using glass beads, in 1 ml of 0.1 M sodium cacodylate buffer, pH 7.4, at 22°C (3). The newly formed liposomes were then pelleted by centrifuging at 1,500 *g* for 10 min. The pellet was suspended for 5–60 min in 0.2 or 0.02% digitonin (Sigma Chemical Co.) or in 1.5% glutaraldehyde and buffer, with or without added 0.2% digitonin (21, 42), and processed for freeze-fracture or embedding in Epon (see below).

LIVER: Livers were excised from mice under ether anesthesia, diced into 1-mm^3 pieces, and washed three times with ice-cold 0.9% sodium chloride solution. The tissue cubes were divided into three equal portions (≃1 g each), weighed, and processed generally according to Scallen and Dietert (47) and as detailed in Table I. Sample 1 was immersed in 1.5% glutaraldehyde containing 0.2% digitonin and 1% sucrose in 0.1 M sodium cacodylate buffer for 16 h at room temperature. Sample 2 was fixed in buffered glutaraldehyde without added digitonin. Sample 3 was extracted directly in chloroform-methanol (reagents redistilled, 2:1, vol/vol; Mallinckrodt Inc., St. Louis, Mo.). After fixation, a few small fragments of samples 1 and 2 were removed for microscopy of freeze-fracture replicas. The remainder was washed three times in 0.1 M cacodylate buffer containing 7% sucrose, postfixed in 1% osmium tetroxide in 0.1 M cacodylate buffer, dehydrated in graded ethanols, and immersed in Epon for 24 h. After removal of a small sample for routine embedding, most of the tissue was retrieved from the Epon mixture, homogenized in 40 ml of chloroform-methanol (2:1, vol/vol), and allowed to stand for 16 h at 4°C. The solvent was filtered (Whatman No. 43; Whatman, Inc., Clifton, N. J.), dried under 100% nitrogen, resuspended in absolute isopropanol (Eastman Organic Chemicals Div., Rochester, N. Y.) (47), and assayed for cholesterol and triglycerides (35).

UPPER EPIDERMAL SHEETS: To measure cholesterol retention at the time of freeze-fracture, and to determine the effect of fixation time on sterol retention, we divided 100–200-mg aliquots of the upper epidermal sheets freshly obtained from neonatal mice (18) into four equal batches. These were then weighed and fixed

TABLE I

*Digitonin Protocol: Controls and Methods for In Situ Precipitation of Cholesterol**

Fixative + Digitonin	Fixative alone	Unfixed control (no digitonin)
1. 1.5% glutaraldehyde + 0.2% digitonin – fix 16 h	1. 1.5% glutaraldehyde – fix 16–20 h	1. Extracted with chloroform-methanol-water (1:2:0.8, vol/vol/vol) (40 ml/g), homogenize, shake, filter, dry under N_2, resuspend in isopropanol.
2. Washed – 0.2 M cacodylate buffer		2. Assayed for cholesterol‡
3. Tissue removed for freeze-fracture		
4. Postfixed – 1% OsO_4 in 0.1 M cacodylate buffer		
5. Ethanol dehydration		
6. Epon infiltration × 24 h		
7. Tissue removed for thin-section electron microscopy		
8. Epon removed – 100% acetone, four changes × 5 min		
9. Tissue extracted with chloroform-methanol-water (2:4:1.6, vol/vol/vol) (40 ml/g). Homogenize, shake, filter, dry under N_2, resuspend in isopropanol		
10. Assayed for cholesterol‡		

* Tissue slices or cubes washed three times with 0.9% sodium chloride and filtered through cheesecloth; residual tissue divided into three portions (1–2 g each) and processed as described above.

‡ Cholesterol assayed by modification of the Liebermann-Burchardt method on autoanalyzer (see Materials and Methods).

in glutaraldehyde with 0.2% digitonin, or in glutaraldehyde alone, for either 2 or 16 h. A few fragments were removed for freeze-fracturing and processing for thin sections, and the remainder was homogenized, extracted and analyzed for cholesterol and triglyceride, as with the liver.

SKIN, ADRENAL GLAND, AND EPIDIDYMIS: Samples of mouse skin and adrenal gland and guinea pig epididymis were minced into 1-mm^3 pieces and fixed in glutaraldehyde either with or without 0.2% digitonin. After 16 h of fixation, specimens were divided for freeze-fracture or for processing for thin sections.

GUINEA PIG SPERMATOZOA: Spermatozoa were removed from the caudae epididymides and vasa deferentia of three mature, 600-g, ether-anesthetized animals. The sperm were placed in a fixative solution containing 1.5% glutaraldehyde, 0.1 M sodium cacodylate buffer, and 0.2% digitonin (pH 7.4), or in cacodylate-buffered digitonin only at 22°C. Fixation proceeded either at room temperature for 2 h or at 4°C for 16 h. Cells immersed in buffered digitonin only were treated similarly. After fixation, cells were then pelleted and processed by routine methods for thin-sectioning or freeze-fracture, to be described.

ERYTHROCYTES: Samples of human erythrocytes and erythrocyte ghosts were each divided into three aliquots. Two aliquots of each were fixed for 2 h with either glutaraldehyde and digitonin (sample 1) or glutaraldehyde alone (sample 2). The third aliquot was extracted directly with chloroform-methanol (2:1, vol/vol) and processed as described below (Table I). After removal of a small portion of the fixed tissue (samples 1 and 2) for freeze-fracture and embedding, the remaining cells were extracted with chloroform-methanol, and processed for cholesterol and triglyceride determinations, as detailed below.

Freeze-Fracture and Electron Microscopy

Tissues for freeze-fracture were immersed in buffered glutaraldehyde, glutaraldehyde plus digitonin, or digitonin. They were then infiltrated with 25% glycerol in 0.1 M cacodylate buffer for 2 h, mounted on cardboard disks, and frozen in liquid nitrogen after brief quenching in Freon (E. I. du Pont de Nemours & Co., Wilmington, Del.) at −150°C. Specimens were then fractured and shadowed with platinum-carbon at −115°C in a freeze-etch apparatus (Balzers High Vacuum Corp., Santa Ana, Calif.). Replicas were cleaned sequentially with absolute methanol and Chlorox. Liposomes were handled in the same manner, but infiltrated with 40% glycerol in 0.1 M cacodylate buffer and frozen in suspension directly onto the Balzers specimen stage before fracture.

Tissue specimens and cell suspensions destined for thin-sectioning were dehydrated in graded acetone solutions and embedded in Epon. Liposomes were processed similarly except that they were stained en bloc with tannic acid as recently described (23). All sections were cut with diamond knives and stained with lead citrate and uranyl acetate. Sections and replicas were examined in either a Philips 201 or Siemens 101 electron microscope at accelerating voltages of 60 or 80 KV.

Lipid Extraction and Analysis

Cholesterol was extracted and analyzed by a modification of the method of Scallen and Dietert (47). As detailed above, aliquots of tissue were taken both before and after fixation. Tissues were extracted with chloroform-methanol-water (1:2:0.8; vol/vol/vol) (40 ml/g wet weight) in a ground-glass homogenizer (6), and agitated at 6 cycles/s for 10 min with a modified wrist-action shaker (Burrell Corp., Pittsburgh, Pa.). Two phases were produced by adding unit volumes of chloroform and water; the upper phase was washed twice with clean lower-phase solvent. Combined lower phases were filtered through solvent-extracted Whatman No. 43 paper, dried under nitrogen, resuspended in absolute isopropanol, and stored at −20°C. Samples were then analyzed for cholesterol (as total sterol) and triglyceride in an autoanalyzer (35). To remove resin, Epon-infiltrated specimens were washed four times for 5 min with 100% acetone (Mallinckrodt reagent), then extracted and processed as described above.

RESULTS

Cholestrol Assay during Fixation and Embedding

ERYTHROCYTE GHOSTS: Almost 100% of erythrocyte ghost cholesterol was retained in membrane pellets during 2-h fixation in glutaraldehyde plus digitonin, but only 60% was retained when digitonin was omitted. Table II gives the results of two such experiments. It should be noted that the retained cholesterol component reflects precipitation of cholesterol in general, not solely that within membranes, since microscopy revealed that sterol-digitonide complexes were progressively removed from membranes.

UPPER EPIDERMAL SHEETS: In these experiments and in experiments with liver, the specificity of the digitonin reaction for cholesterol was checked by comparing cholesterol and triglyceride retention. Assays were performed both before and after fixation, and during the final stages of Epon embedding. Table III presents averaged results from two experiments: tissue treated for 2 h with digitonin retain ~60% of cholesterol noted in control samples; prolonging digitonin treatment to 16 h resulted in >80% retention. Fixation in glutaraldehyde alone was ineffective in retaining cholesterol. Triglycerides were extracted during processing regardless of digitonin's inclusion in the fixative.

LIVER: Digitonin-glutaraldehyde fixation retained 43% of cholesterol and only 2% of triglycerides originally present in the liver samples (Table IV). Since chloroform-methanol extraction of complexed cholesterol is incomplete after fixation and embedding, these cholesterol percentages are likely to be conservative. Additional treatment with dimethylsulfoxide is often required to assess total tissue cholesterol retention (47).

TABLE II

*Effect of Digitonin on Cholesterol Retention in Pellets of Erythrocyte Ghosts**

	Pellet		Supernate	
	μM/g	*(%)‡*	*μM/g*	*(%)‡*
Erythrocyte ghost control	.357	(100)	–	–
Erythrocyte ghosts + glutaraldehyde	.347	(97)	.02	(5)
Erythrocyte ghosts + glutaraldehyde alone	.219	(61)	.08	(29)

* Pellets of freshly prepared erythrocyte ghosts, previously exposed to glutaraldehyde alone or to glutaraldehyde plus digitonin, were extracted directly with chloroform-methanol-water (see Materials and Methods). Supernates were extracted by adding chloroform and methanol to buffer in same ratio. Washing, resuspension, and cholesterol assay of both pellets and supernates were performed as described in Materials and Methods.

‡ Average percent retained in two experiments.

TABLE III

*Effect of Digitonin on Retention of Triglycerides and Unesterified 3-β-Hydroxysterols in Neonatal Mouse Stratum Granulosum and Corneum**

		Glutaraldehyde + digitonin				Glutaraldehyde alone			
	Control	2 h		16 h		2 h		16 h	
	mg/g wet wt	*mg/g wet wt*	*(%)‡*	*mg/g wet wt*	*(%)‡*	*mg/g wet wt*	*(%)‡*	*mg/g wet wt*	*(%)‡*
Cholesterol	9.9	5.1	(60)	8.1	(82)	1.1	(11)	0	(0)
Triglycerides	17.8	0	(0)	Not done		0.17	(1)	Not done	

* Controls were directly extracted with chloroform-methanol (2:1, vol/vol). Cholesterol and triglycerides were also assayed simultaneously in autoanalyzer (see Materials and Methods).

‡ Average percent retained in two experiments.

TABLE IV

*Effect of Digitonin on Retention of Hepatic Triglycerides and Unesterified 3-β-Hydroxysterols**

	Control	Glutaraldehyde + digitonin		Glutaraldehyde alone	
	mg/g wet wt	*mg/g wet wt*	*(% retained)*	*mg/g wet wt*	*(% retained)*
Cholesterol	4.8	2.1	(43)	0.13	(2.6)
Triglycerides	42.8	1.0	(2.4)	0.6	(1.4)

* Cholesterol and triglycerides were assayed simultaneously in an autoanalyzer (see Materials and Methods).

Multilamellar Liposome Morphology

No differences were seen between plain phosphatidylcholine liposomes exposed to digitonin and cholesterol-containing liposomes not exposed to digitonin in either thin sections or freeze-fracture replicas (Figs. 1–3). In contrast, cholesterol-containing liposomes treated with digitonin developed corrugations and tubular complexes within and adjacent to membranes (Figs. 4–7). The number of extraliposomal complexes increased with the duration of digitonin treatment and with increased concentrations of digitonin (from 0.02 to 0.2%). In all experiments, both the tubular complexes and corrugations were ~50–60 nm in width, of variable length, and identical in size and configuration to those in cells and tissues (cf. Figs. 13, 19, 21, and 23). In thin sections, many tubular complexes consisted of an amorphous, perhaps empty, core, 50 nm in width (Figs. 5 and 6), which consistently cross-fractured in freeze-fracture preparations (Fig. 7). The central core was, in turn, surrounded by a single thin lamina, and a small portion of tubules were also enveloped partially by typical bilayer membrane structures (Figs. 5–7). Because freeze-fracture replicas of digitonin-treated crystalline cholesterol revealed only the core structure without the surrounding outer trilaminar shell (Figs. 8 and 9), the latter structure may represent residual, reorganized phosphatidylcholine bilayers consequent to cholesterol stripping.

During the first hour of digitonin treatment, most of the liposomes were replaced by tubular complexes; only a few intact liposomes remained. Cholesterol removal occurred quickly since hemitubular complexes were almost always found adjacent to, but only occasionally within, fractured liposomal membranes (Figs. 4 and 5). When encountered within liposomes, there were equal proportions of convex and concave fracture-faces.

Moreover, the ratio of phosphatidylcholine to cholesterol within liposomes did not influence the outcome: liposomes composed of varying mole ratios of phosphatidylcholine to cholesterol (5:1, 2:1, or 1:1) were all rapidly transformed into tubular complexes. Glutaraldehyde did not affect the result. The complexes were generally of the same width but of varying length which was independent of treatment times. Hemitubular complexes appeared in mixtures of purified cholesterol and digitonin (Figs. 8 and 9), indicating that no other lipids are needed for their formation.

Tissue Morphology

When solid tissues were immersed in digitonin before or even during glutaraldehyde fixation, extensive damage occurred. The extent of membrane disruption differed from tissue to tissue, and from level to level within each specimen, presumably because of different rates of penetration by digitonin and fixative. Although glutaraldehyde fixation before exposure to digitonin prevents much of the damage, it heightens the tendency to induce cross-fractures, a disturbance already enhanced by digitonin.

EFFECTS ON ORGANELLE MEMBRANES IN LIVER, ADRENAL GLAND, SKIN, AND EPIDIDYMIS: In general the plasma membranes of fractured stromal fibroblasts and endothelial cells corrugated uniformly (Fig. 10); but within epithelia this modification was more patchy and irregular, revealing a mosaic of unperturbed domains as well as regions of densely packed, elongated corrugations (Figs. 11 and 12). The number of corrugations on freeze-fractured P-face images was not substantially different from that on E-face images.

The corrugations in digitonin-treated plasma membranes were all of the same width (50–60 nm) and coursed in parallel, swirling, anastomosing arrays (Figs. 10 and 12). These corrugations were similar in length, width, and configuration to those formed in digitonin-treated liposomes and to those found outside of membranes in digitonin-treated tissues (Figs. 13 and 14). In P-face images, they appeared as tightly packed, tubular convexities separated by a narrow groove (Fig. 12); on E faces, they comprised corresponding concavities (Figs. 10 and 15); that is, when adjacent E- and P-face corrugations were compared, it was evident that the images were complementary.

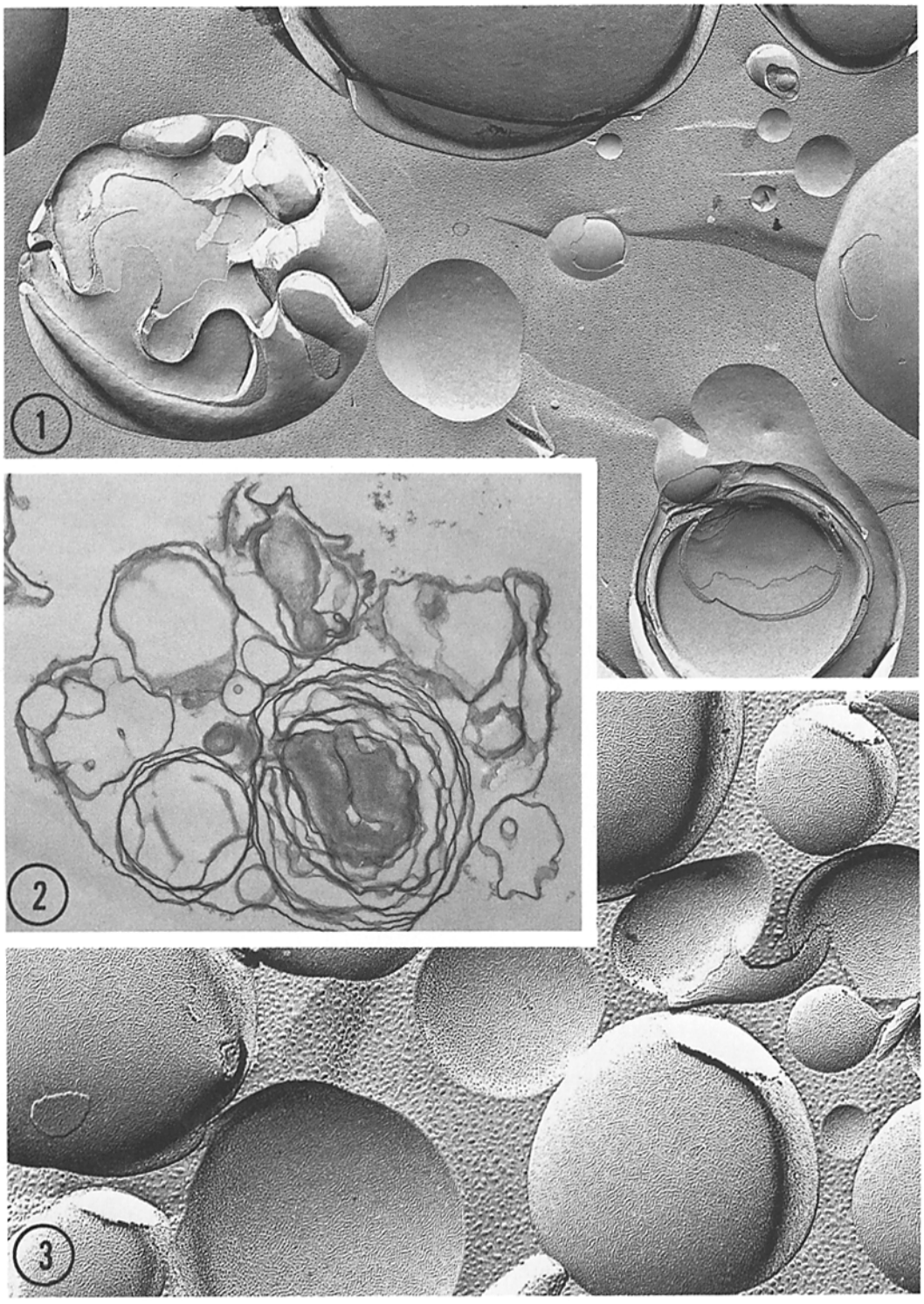
1
2
3

In addition, intracellular corrugations were also seen frequently in lysosomes and in some Golgi complex-derived vesicles (Figs. 16 and 17), whereas nuclear and mitochondrial envelopes were only minimally perturbed (Figs. 15, 16, and 18). Other intracellular organelles, such as endoplasmic reticulum and Golgi cisternae, tended to cross-fracture so that comparisons in freeze-fracture replicas were not possible.

HETEROGENEITY OF CHOLESTEROL DISTRIBUTION WITHIN INDIVIDUAL EPITHELIAL PLASMA MEMBRANES: In addition to their "patchy" character within epithelial plasma membranes, corrugations did not impinge on domains occupied by gap junctions or tight junction strands (Figs. 20–22) in any epithelia studied. Moreover, corrugations invariably crossed regions where particle-poor halos surrounded gap junctions, but stopped abruptly at the edge of rectilinear arrays (Fig. 20). Most desmosomes, except those in epidermis (a keratinizing epithelium), were regularly traversed. This sparing effect on tight- and gap-junction regions was particularly pronounced in some thin-sectioned fields, where only the cell junctions escaped destruction (Fig. 22). Coated plasma membrane invaginations and coated vesicles were also spared by digitonin in all the epithelia studied (Fig. 23).

Isolated Cell Morphology

Because the heterogeneous distribution of cholesterol-digitonin complexes within epithelial plasma membranes could be ascribed to uneven tissue penetration through junctions, we sought to circumvent this obstacle by exposing suspensions of sperm and erythrocytes to digitonin.

GUINEA PIG SPERMATOZOA: After incubation in digitonin, the plasma membrane of the guinea pig spermatozoon corrugated uniformly (Figs. 24–29), except for two areas of the tail: the annulus (Figs. 28 and 29), which separates the mitochondrion-rich midpiece from the principal piece, and the zipper, which courses lengthwise, opposite fiber 1 (Fig. 27). The striated ring dividing the head and tail also remained unfurrowed, whereas parts of the head plasma membrane overlying the acrosomal cap and the equatorial segment (Figs. 24–26) appeared corrugated (Fig. 24*a*). The membrane of the acrosomal cap itself scalloped extensively (Fig. 25), but neither the inner portion of the acrosomal membrane comprising the equatorial segment (Fig. 26) nor the nuclear envelope corrugated at all.

HUMAN WHOLE ERYTHROCYTES AND ERYTHROCYTE GHOSTS: Digitonin incubation, with or without glutaraldehyde, produced extensive degradation of erythrocyte plasma membranes. Characteristic corrugations appeared transiently in some treated whole erythrocytes (Figs. 21 and 32*a* and *b*), but were no longer detectable by freeze-fracture and thin-sectioning as digitonin incubation was extended beyond 120 min and progressively disrupted the membranes (Figs. 33*c*, 34, and 35). Tubular complexes (50–60 nm),

Key to Symbols

A,	annulus	*IAM*,	inner acrosomal membrane
C,	canaliculus	*M*,	mitochondria
CV,	coated vesicles	*N*,	nucleus
E,	E fracture-face	*OAM*,	outer acrosomal membrane
ECM,	extracellular matrix	*P*,	'P' fracture-face
G,	golgi complex	*PM*,	plasma membrane
GJ,	gap junction	*V*,	secretory vesicle

FIGURES 1–3 Control multilamellar liposomes. Shadowing angle in all freeze-fracture illustrations is from the bottom toward the top, except in Fig. 1 which is shadowed from the top downward. Liposomes in Fig. 1, composed of phosphatidylcholine and cholesterol (mole ratio 2:1), were treated with glutaraldehyde and buffer, but without digitonin. Note that vesicles may exhibit single or multiple planes. Liposomes in Fig. 2 are from the same sample as those in Fig. 1. Liposomes in Fig. 3, composed of phosphatidylcholine alone, were treated with glutaraldehyde, buffer, and digitonin. In neither sample is corrugation evident, though both samples exhibit on freeze-fracture a fine pattern of surface irregularity consistent with previously reported pretransitional reorganization patterns related to the rate of freezing the lipid (56). Fig. 1, × 20,000; Fig. 2, × 26,500; Fig. 3, × 45,500.

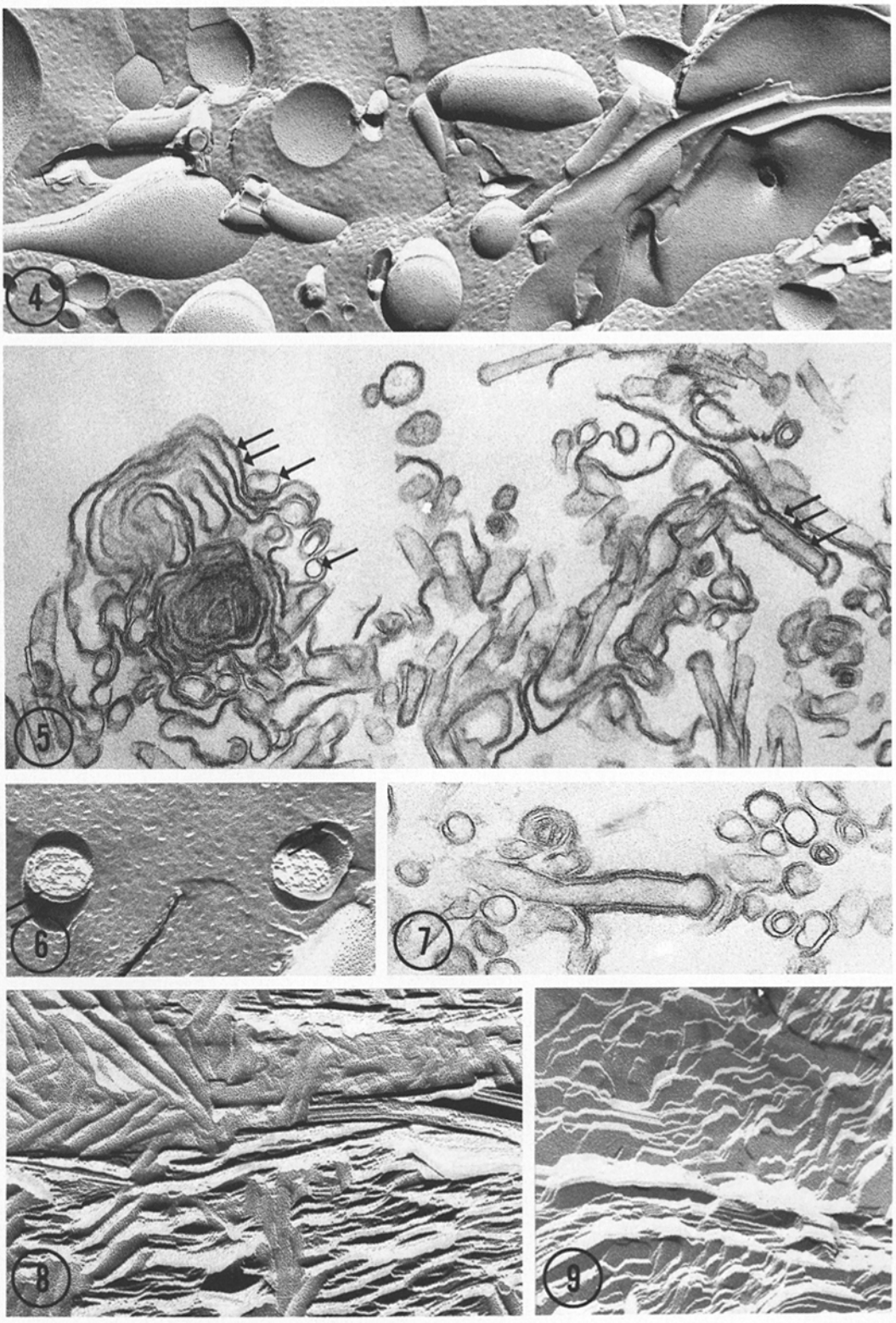
4
5
6
7
8
9

similar to those found in other digitonin-treated tissues and liposomes, appeared adjacent to fragmented cell remnants. In contrast to whole erythrocytes, however, erythrocyte ghosts exposed identically did not exhibit corrugations (Figs. 34–36), suggesting either that the cholesterol content of ghosts was much lower than that of whole erythrocytes, or that ghost cholesterol was more readily removed by digitonin.

In both erythrocytes and erythrocyte ghosts, digitonin incubation induced changes in the organization of integral membrane particles. The usual random freeze-fracture array of intramembrane particles (Fig. 34) was lost, and, instead, particles aggregated into clusters connected by narrow rows (Figs. 32 and 36) with intervening areas of membrane devoid of particles. Clustering occurred as readily in erythrocytes incubated with both digitonin and glutaraldehyde (P. M. Elias, J. Goerke, and D. S. Friend. Unpublished observations) but we have not tested glutaraldehyde fixation before digitonin exposure. The entire fractured leaflet revealed a subtle faceting equally evident in P- and E-face images (Figs. 32, 33, and 36). Polygonal buckling was often more pronounced in ghosted erythrocytes than in whole erythrocyte membranes (cf. Fig. 35 with Fig. 31*c*), a pattern that cannot be ascribed to impingement of extracellular ice, since ice crystal formation was not apparent in our replicas (Figs. 32, 33, and 36). In P fracture-face images, it was evident that both individual particles and particle clusters tended to align along membrane angulations (Figs. 32 and 36).

DISCUSSION

Digitonin Cytochemistry

Digitonin complexes with most unesterified 3-β-hydroxysterols, including cholesterol, the principal free sterol present in vertebrate tissues. Since the molecular weight of digitonin is about three times that of cholesterol, it is not unreasonable that the intercalation of digitonin into cell membranes could produce significant physical alterations within the bilayer. What factors govern the convex/concave pattern of scalloping? One can speculate that it is related to: (*a*) differences in the phospholipid (4), protein (32, 52), or cholesterol composition (20) of the inner vs. outer membrane leaflets, or (*b*) structural constraints imposed by other membrane and extramembrane constituents, e.g., the subplasmalemmal filamentous network (41, 52, 58). Where structural limitations and compositional differences are probably absent, as in the liposome preparations reported here, convexities and concavities appear on both faces, an observation which does not help to distinguish between these possibilities.

Additional information about the digitonin-cholesterol complex can be gleaned from experiments with liposomes. Because glutaraldehyde had no effect on the morphology or rate of digitonin-cholesterol complex formation, we can conclude that glutaraldehyde may be used in future investigations to improve preservation of tissues. Moreover, since tubular forms are seen with pure cholesterol, there is no a priori requirement that the sterol be organized within a membrane or

FIGURES 4–7 Multilamellar liposomes composed to phosphatidylcholine and cholesterol (mole ratio 2:1), treated with 0.2% digitonin. Elongated tubules or cylinders of constant width (50–60 nm), but variable length, appear as liposomes are distorted and degraded. Each tubular complex comprises a slightly electron-opaque core surrounded by a single leaflet, seen best in cross sections (Figs. 5 and 6, single arrows). Occasionally, tubular complexes are encircled by an additional bilayer (Figs. 5 and 6, double arrows). In freeze-fracture specimens, the tubule cores cross-fracture, and are cuffed by one or two lamellae (arrows), which may represent the membranes seen in corresponding thin sections (Figs. 5 and 6). Fig. 4, × 58,000; Fig. 5, × 68,500; Fig. 6, × 79,000; Fig. 7, × 92,000.

FIGURES 8 and 9 Crystalline cholesterol treated with buffer (Fig. 8) or with buffer and 0.2% digitonin (Fig. 9). After 20 min of digitonin treatment, hemicylindrical structures often traverse crystals in parallel arrays at acute angles to underlying crystal fracture planes (Fig. 9). Hemitubules are 50–60 nm wide and are identical in dimension and configuration to the tubular complexes formed in digitonin-treated phosphatidylcholine-cholesterol liposomes, except that additional membrane bilayers are not found (cf. Figs. 5–7). Fig. 8, × 52,000; Fig. 9, × 82,500.

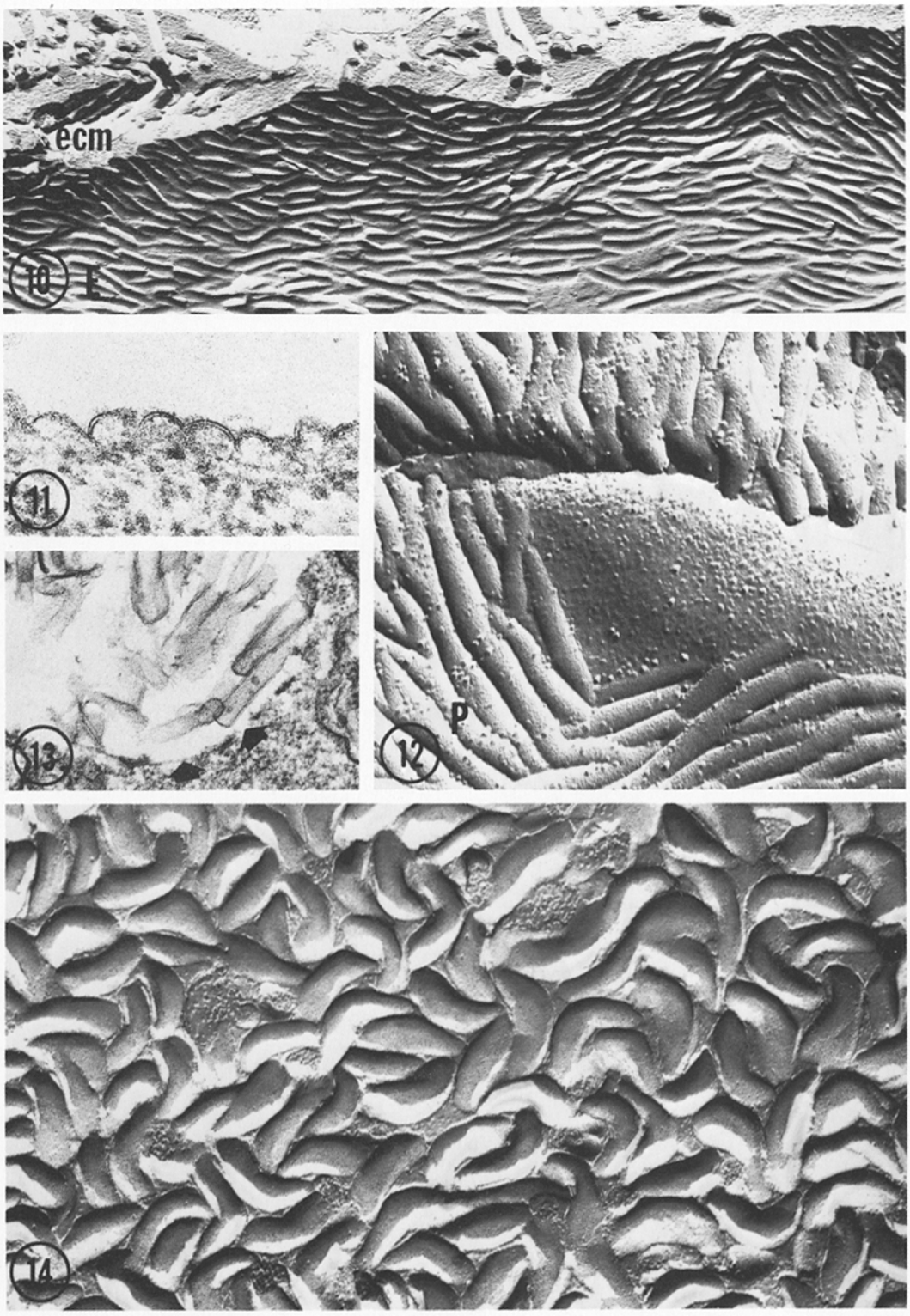
ecm
10
E
11
13
P
12
14

mixed with other lipids. This model system also indicates that the size and shape of tubular complexes is determined by the complexing of cholesterol and digitonin and not by other structural or chemical constraints. The core of each complex is enclosed first by a unilaminar leaflet, and then variably cuffed by a membrane bilayer when phospholipid is present. We speculate that digitonin-cholesterol complexes form the core of these structures, and that the polar ends of cholesterol or digitonin molecules may react with osmium to produce the narrow, outer electron-opaque layer. The variably present outer membrane may then represent phosphatidylcholine bilayers.

It seems clear that the presence of tubular complexes in digitonin-exposed freeze-fracture replicas can provide a useful morphological marker for the presence of cholesterol in membranes (19, 38). Since processing for freeze-fracture is less disruptive than processing for thin-sectioning, the digitonin method should prove more reliable in this setting. Despite considerable quantitative evidence that cholesterol is retained within tissues after digitonin treatment (1, 39, 40, 46, 47, 60), this technique has important drawbacks. Digitonin is a powerful detergent, capable of solubilizing membrane constituents, even when application is preceded (59) or accompanied by (21, 42, 47) aldehyde fixation. This effect, largely ignored in the cytochemical literature, makes precise quantitative studies on *in situ* retention difficult. Although quantitative retention of cholesterol has been demonstrated here and in earlier studies (47), it has not been possible to differentiate between cholesterol in extramembrane precipitates and cholesterol in its original membrane site.

Variations in Cholesterol Composition between Organelle Membranes

Freeze-fracture replicas of digitonin-exposed cells and tissues reveal striking variations in corrugations between different organelles. In all cell types studied, the plasma membrane was heavily convoluted, whereas nuclear, mitochondrial, Golgi complex, and rough endoplasmic reticulum envelopes were only rarely perturbed. This pattern is consistent with the known cholesterol content of these organelles, the former containing considerably more cholesterol than any of the latter (11, 29, 31, 33, 54). The lack of corrugations within some organelle membranes may be due to their tendency to cross-fracture, independent of digitonin exposure. Certain Golgi complex- and endoplasmic reticulum-derived structures, such as lysosomes and epidermal lamellar body membranes, were uniformly plicated. Lysosomes are known to be relatively cholesterol-rich (29, 54) and lamellar bodies contain large quantities of free sterols (17).

Intramembrane Variations in Cholesterol Content

Although digitonin freely corrugates and even

FIGURE 10 Freeze-fracture replica of digitonin-treated skin fibroblast surrounded by extracellular matrix. Stromal cell plasma membranes tend to be uniformly plicated. E faces display predominantly concave corrugations packed into parallel, anastomosing valleys 50–60 nm in width; P faces reveal complementary convex, hemitubular corrugations (cf. Fig. 12). × 37,500.

FIGURES 11 and 12 Freeze-fracture replica and corresponding thin section of digitonin-treated keratinocyte plasma membranes. The scalloped appearance of digitonin-treated plasma membranes in thin sections is shown in Fig. 11. In contrast to stromal cells (cf. Fig. 10), epithelial plasma membranes display a patchy distribution of corrugated and noncorrugated regions. P faces display convexities 50–60 nm wide (Fig. 12), and E faces reveal comparable concavities (not illustrated). Note that integral membrane particles are not laterally displaced into grooves between convexities (Fig. 12). Fig. 11, × 108,500; Fig. 12, × 71,000.

FIGURES 13 and 14 Freeze-fracture replica and corresponding thin section of hepatocyte plasma membranes. Extracellular corrugations and tubular complexes predominate if digitonin treatment is prolonged (here, 16 h), or if tissues are not simultaneously fixed or pre-fixed in glutaraldehyde. Note regions of membrane lysis in Fig. 13 (arrows), and smooth, short, particle-free surfaces of fractured extracellular tubular complexes in Fig. 14. Fig. 13, × 66,000; Fig. 14, × 45,000.

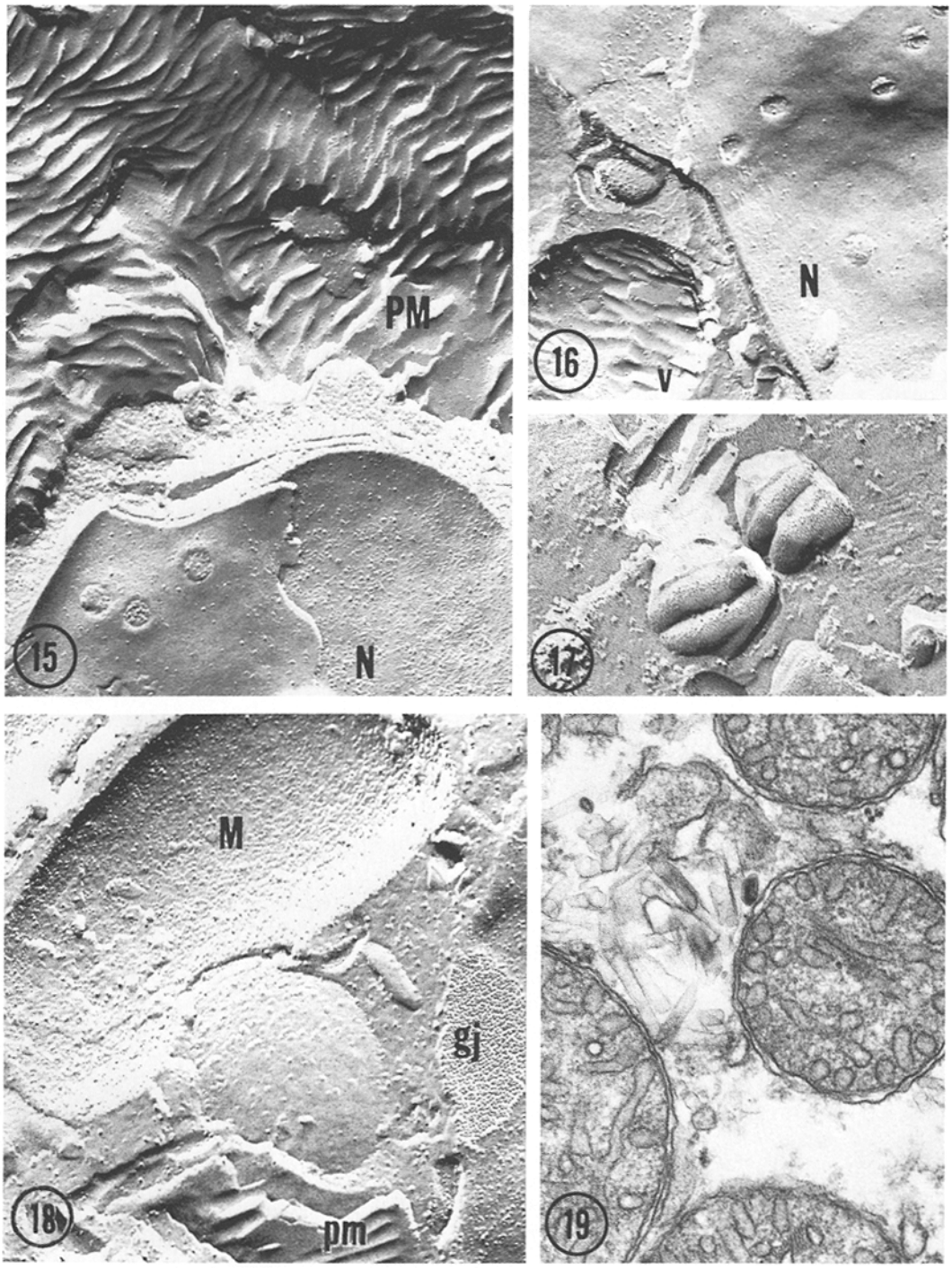

FIGURES 15–19 Digitonin-treated epithelial plasmalemmal and intracellular organelle membranes. Plasma membranes are invariably plicated, though in a non-uniform manner (Fig. 18; cf. Fig. 12), as are some vacuolar and secretory organelle membranes (Figs. 16 and 17). In contrast, nuclear (Figs. 15 and 16) and mitochondrial (Figs. 18 and 19) envelopes are rarely corrugated. Occasionally, after lysis of the plasma membrane, the cell cytoplasm is disrupted but the mitochondria seem to float unperturbed (Fig. 19). Fig. 15 (liver), × 58,500; Fig. 16 (liver), × 58,000; Fig. 17 (epidermis), × 87,500; Fig. 18 (liver), × 59,500; Fig. 19 (adrenal gland), × 38,000.

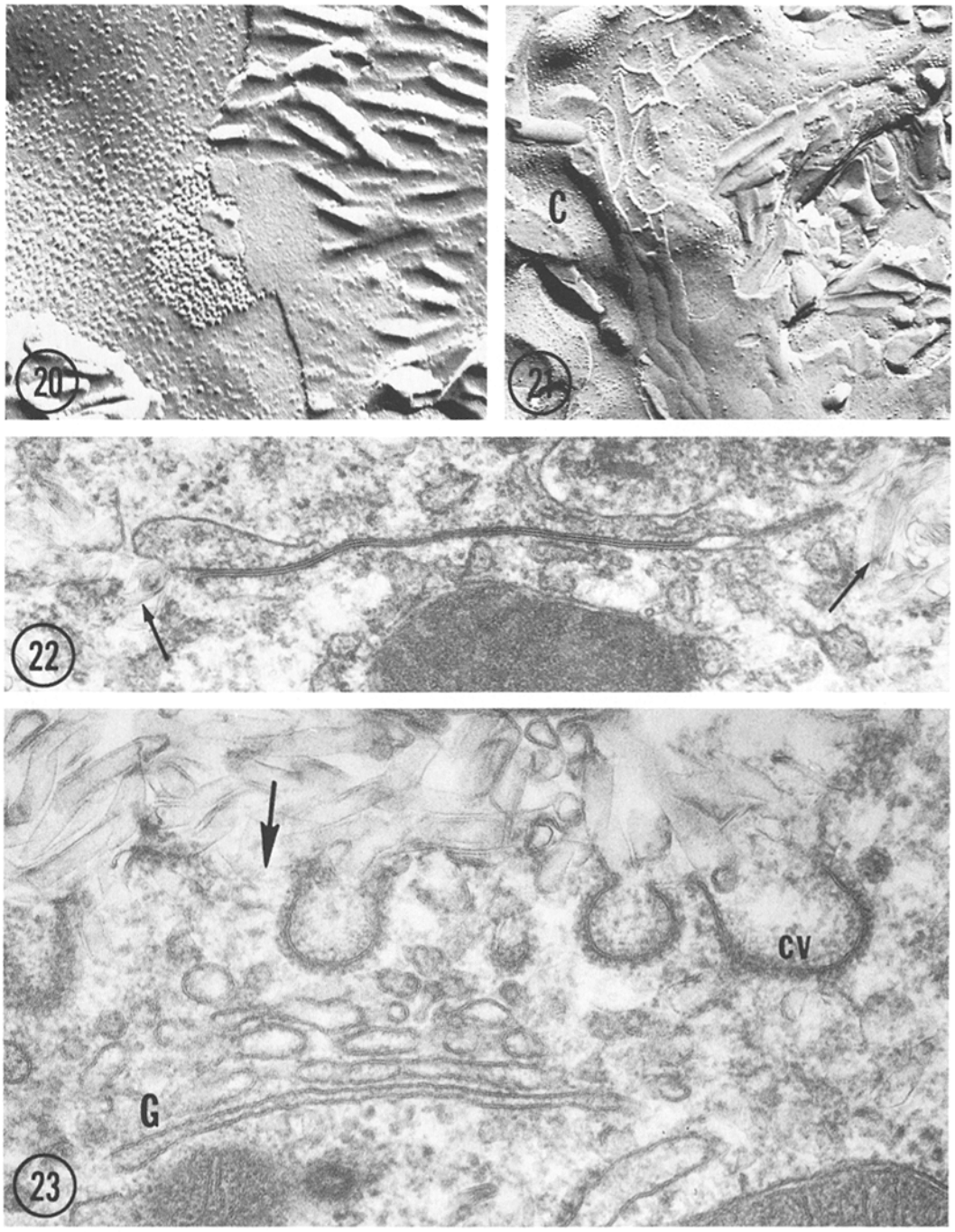

FIGURES 20–23 Digitonin-treated hepatocyte plasma membranes. Gap junctions are spared by corrugations which often abut directly on orthogonal particle clusters (Fig. 20). In more exhaustively treated specimens, the entire surrounding membrane may be lysed (arrows), yet the gap junction still appears unaffected (Fig. 22). Tight junctions are similarly spared; corrugations may approach, but do not distort, the most basal strand, even when the adjacent membrane is extensively damaged, as in Fig. 21 (note the particle-free extracellular tubular complexes to the right). More apical strands, as well as plasma membrane regions lining canaliculi, are not plicated, possibly due to poor penetration of digitonin through the junction. Coated vesicles are like-wise left intact, even in regions of extensive membrane lysis (Fig. 23, arrows). Note the sparing of Golgi membranes as well (cf. Figs. 18 and 19). Fig. 20, × 71,500; Fig. 21, × 61,500; Fig. 22, × 33,500; Fig. 23, × 47,500.

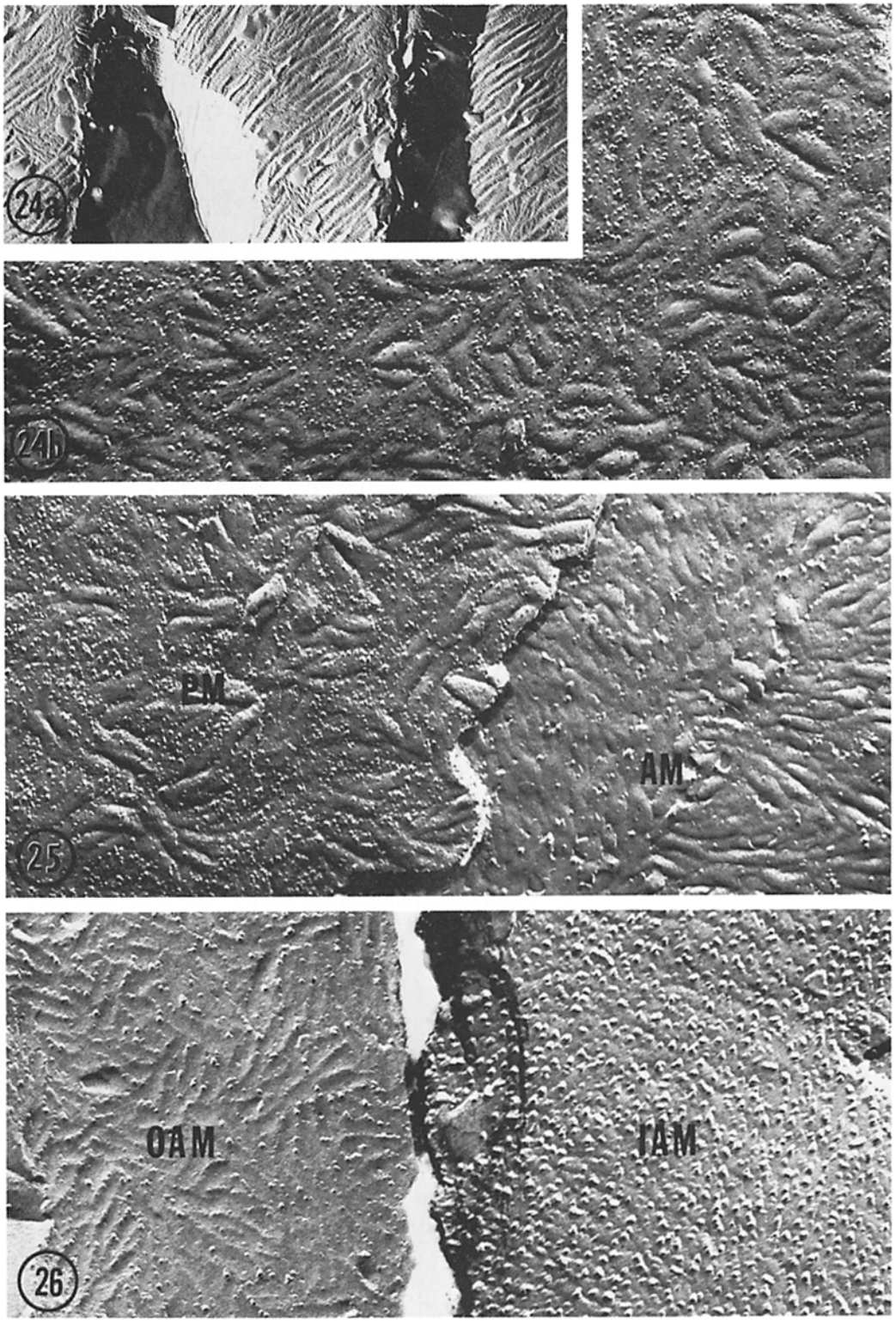
24a
24b
PM
AM
25
OAM
IAM
26

disrupts large portions of the plasma membrane of most epithelia, it does not attack gap junctions, tight junctions, or coated vesicles. Limited data are available on the lipid composition of these plasma membrane specializations, but they are consistent with the failure of these structures to corrugate. For example, a recent study indicates that gap-junction regions are deficient in neutral lipids (26). Similarly, the failure of coated vesicles to corrugate may indicate that the membrane is sterol-poor, incompletely permeated, or too rigid to fold at these sites. The recent work of Pearse indicates that these regions contain a low phospholipid:protein ratio and a very low proportion of cholesterol (44); thus, as with gap junctions, this may explain why they remain intact when the remainder of the membrane surface is either disrupted or depleted (8).

Tight-junction strands and interstrand membrane regions also do not corrugate, but the general failure of the interstrand regions to become folded may reflect incomplete penetration by digitonin rather than actual regional deficiencies in sterol. This interpretation is supported by our observation that the luminal plasma membrane of liver is usually not corrugated when the subjacent tight junction is not corrugated. No data exist, as yet, on the composition of tight-junction strands and interstrand membrane regions.

SPERM: Sperm membranes demonstrate the same distribution of organelle membrane folding as is found in solid tissues; unfortunately, little is known about the lipid composition of different sperm membranes (9). Of more interest is the heterogeneity of the corrugations observed within the plasma membrane of sperm, for these corrugation differences cannot be ascribed to unequal penetration of digitonin and/or fixative. The plasma membrane of the sperm head, though uniformly plicated, corrugates in parallel arrays at an angle to the long axis (Fig. 24*a*). Heterogeneity is also observed within tail plasma membranes, where the annulus and zipper regions do not convolute, but the remainder of the membrane is either corrugated or lysed. Exposure of spermatozoa to digitonin, without added glutaraldehyde, progressively degrades the membrane. Inasmuch as the initially unfurrowed regions are not attacked, digitonin may provide a useful means for the systematic separation and isolation of these spared portions (22). Exploiting this selective action of digitonin may also provide an alternate method for isolation of gap and tight junctions and coated pits in other tissues.

Erythrocytes

Intact erythrocytes and erythrocyte ghosts respond to digitonin in a manner quite different from that of sperm and solid tissues. Corrugations are encountered only transiently in the exposure of whole erythrocytes, and not at all with ghosts. Simultaneous glutaraldehyde fixation does not prevent the rapid formation of extracellular digitonin-cholesterol complexes in either case. One can speculate that the cholesterol thus removed corresponds to the readily exchangeable pool described by several investigators (10, 34), but only detailed isotope exchange experiments can provide an answer. If such experiments were to show that erythrocyte isolated from digitonin-extracted cholesterol still contained substantial amounts of nonradioactive cholesterol, it would provide further evidence for the existence of two membrane pools of this compound. The absence of membrane corrugations in digitonin-exposed ghosts may lend support to those (55) who claim that the ghosting procedure disrupts and even removes membrane cholesterol.

A further difference between erythrocytes and other cells is that digitonin exposure produces

FIGURES 24–26 Various portions of guinea pig sperm head membranes. In Fig. 23*a*, the plasma membranes of three adjacent sperm heads reveal digitonin-cholesterol hemitubular complexes all lying in the same direction. At higher magnification, the digitonin-induced corrugation of the head plasma membrane P face is uniform (Fig. 24*b*). In Fig. 25, the head plasma membrane P face and outer acrosomal membrane E face are corrugated. Note that particles maintain the same random distribution and half-membrane affinity as in glutaraldehyde-fixed controls, but the particles are ≈50% larger than in spermatozoa not treated with digitonin. In Fig. 26, the half membrane (E face) on the left may be the outer acrosomal membrane, but its identity is not certain. The P face of the heavily particulate, inner acrosomal membrane does not corrugate. Fig. 24*a*, × 19,000; Fig. 24*b*, × 75,000; Fig. 25, × 75,000; Fig. 26, × 100,000.

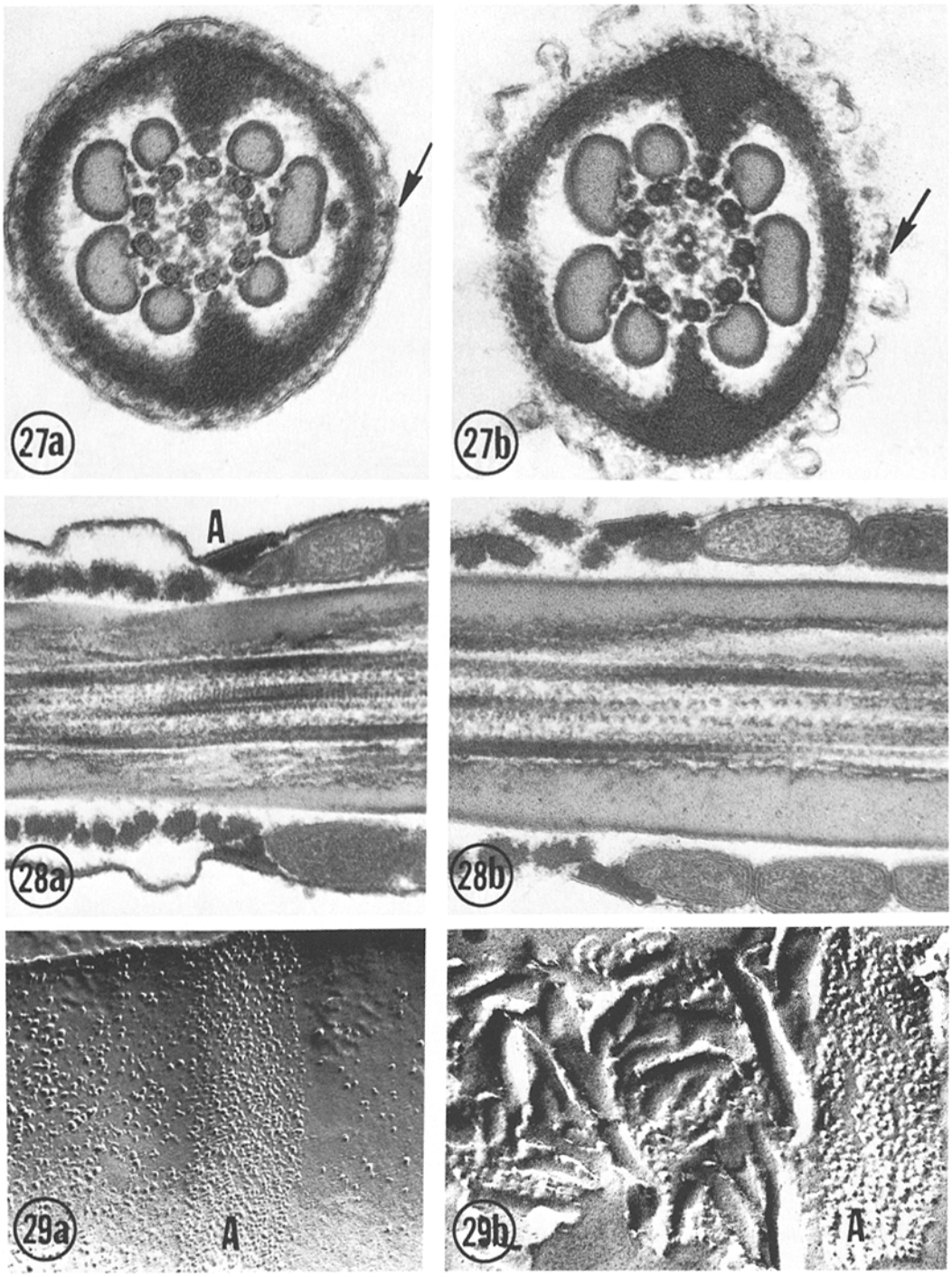

FIGURES 27–29 Various portions of guinea pig sperm tail membranes. Fig. 27*a* and *b* depict cross sections of the principal piece of the sperm tail fixed in tannic acid and glutaraldehyde. The densities (arrows) in the plasma membrane opposite fiber 1 correspond to the "zipper." Digitonin treatment (Fig. 27*b*) scallops the membrane but spares the zipper and a narrow boundary of trilaminar membrane. In Fig. 28*a* and *b*, the annulus, which separates the midpiece (to the right) from the principal piece, is depicted. Digitonin treatment (Fig. 28*b*) scallops the plasma membrane of the midpiece, disrupting it in the principal piece, but spares the membrane of the annulus. Fig. 29*a* and *b* portray regions in freeze-fracture equivalent to those seen in thin sections (Fig. 28). Note that the E face of the annulus is rich in membrane particles. Digitonin treatment corrugates the plasma membrane of the midpiece but does not perturb the annulus. Fig. 27*a*, × 76,000; Fig. 27*b*, × 77,000; Fig. 28*a*, × 58,000; Fig. 28*b*, × 69,000; Fig. 29*a*, × 60,000; Fig. 29*b*, × 114,000.

particle clustering in the former. In addition, residual erythrocyte membranes tend to buckle, presumably at sites of particle aggregation. The association of particle clustering with removal of cholesterol and cholesterol-digitonin complexes from erythrocyte membranes suggests that cholesterol acts to restrict lateral displacement of integral membrane particles in erythrocytes. However, other factors also control integral membrane movement, since protein removal (16, 58), pH changes (45), and lectin agglutination (2) also will induce lateral displacement of erythrocyte integral membrane proteins. Such particle aggregation is identical to that described in freeze-fracture of artifical (37) and natural (14, 28, 38, 51, 61) membranes in which membrane fluidity is experimentally altered by manipulating temperature, fatty acid composition, and cholesterol content.

Figs. 14, 22, and 23 were kindly provided by Dr. Roberto Montessano. The authors gratefully acknowledge the invaluable assitance of Diana Cohen, Vera Vaughn, William Chapman, and Irene Rudolph.

This work was supported by National Institutes of Health grants AM 19098, HD 10445, and HLI 06285, and the Medical Research Service of the Veterans Administration Hospital.

Received for publication 3 January 1978, and in revised form 29 March 1978.

REFERENCES

1. ALBERT, E. N., and R. D. RUCKER. 1975. Electron microscopic demonstration of cholesterol in atheromatous aortae. *Histochem. J.* **7**:517–527.
2. BÄCHI, T., and H. P. SCHNEBLI. 1975. Reaction of lectins with human erythrocytes. II. Mapping of con A receptors by freeze-etching electron microscopy. *Exp. Cell. Res.* **91**:285–295.
3. BANGHAM, A. D. 1972. Lipid bilayers in biomembranes. *Annu. Rev. Biochem.* **41**:753–756.
4. BARGELSON, L. D., and L. I. BARSUKOV. 1977. Topological asymmetry of phospholipids in membranes. *Science (Wash. D. C.).* **197**:224–230.
5. BLADEN, P. 1958. *In* Cholesterol. R. P. Cook, editor. Academic Press, Inc., New York., 15–115.
6. BLIGH, E. G., and W. J. DYER. 1959. A rapid method of total lipid extraction and purification. *Can. J. Biochem. Physiol.* **37**:911–917.
7. BROCKERHOFF, H. 1974. Model of interaction of polar lipids, cholesterol, and proteins in biological membranes. *Lipids.* **9**:645–650.
8. CARPENTIER, J. L., A. PERRELET, and L. ORCI. 1977. Morphological changes of the adipose cell plasma membrane during lipolysis. *J. Cell Biol.* **72**:104–117.
9. CLEGG, E. D., D. J. MOORE, and D. D. LUNSTRA. 1975. Porcine sperm membranes: in vivo phospholipid changes, isolation and electron microscopy. *Biol. J. Linn. Soc.* **7**(Suppl. 1):321–335.
10. COOPER, R. A. 1977. Abnormalities of cell membrane fluidity in the pathogenesis of disease. *N. Engl. J. Med.* **297**:371–376.
11. DALLNER, G., and L. ERNSTER. 1968. Subfractionation and composition of microsomal membranes: a review. *J. Histochem. Cytochem.* **16**:611–632.
12. DEUEL, H. J. J. 1961. *In* The Lipids. L. Zechmeister, editor. Interscience Publishers, Inc., New York. 3:325–3440.
13. DODGE, J. T., C. MITCHELL, and D. J. HANAHAN. 1963. The preparation and chemical characteristics of hemoglobin-free ghosts of human erythrocytes. *Arch. Biochem.* **100**:119–130.
14. DUPPEL, W., and G. DAHL. 1977. Effect of phase transition on the distribution of membrane-associated particles in microsomes. *Biochim. Biophys. Acta.* **426**:289–296.
15. EBERSPACHER, B. E., D. T. ORGANISCIAK, and E. J. MASSARO. 1977. Alterations in lipid composition of liver cell plasma membranes during development. *J. Exp. Zool.* **199**:289–296.
16. ELGSAETER, A., and D. BRANTON. 1974. Intramembrane particle aggregation in erythrocyte ghosts. I. The effects of protein removal. *J. Cell Biol.* **63**:1018–1036.
17. ELIAS, P. M., J. GOERKE, and D. S. FRIEND. 1977. Mammalian epidermal barrier layer lipids: composition and influence on structure. *J. Invest. Dermatol.* **69**:535–546.
18. ELIAS, P. M., P. FRITSCH, G. TAPPEINER, H. MITTERMAYER, and K. WOLFF. 1974. Experimental staphylococcal toxic epidermal necrolysis (TEN) in adult humans and mice. *J. Lab. Clin. Med.* **84**:414–424.
19. ELIAS, P, M., J. GOERKE, and D. S. FRIEND. 1977. Freeze-fracture identification of cell and liposome cholesterol-digitonin complexes. *J. Cell Biol.* **77**:221a (Abstr.)
20. FISHER, K. A. 1976. Analysis of membrane halves: cholesterol. *Proc. Natl. Acad. Sci. U.S.A.* **73**:173–177.
21. FLICKINGER, C. J. 1967. The postnatal development of the Sertoli cells of the mouse. *Z. Zellforsch. Mikrosk. Anat.* **78**:93–113.
22. FRIEND, D. S., and P. M. ELIAS. 1977. Selective solubilization of the zipper and other components of the guinea pig sperm tail. *J. Cell Biol.* **77**:228a. (Abstr.)
23. FRIEND, D. S., L. ORCI, A. PERRELET, and R. YANAGIMACHI. 1977. Membrane particle changes attending the acrosome reaction in guinea pig spermatozoa. *J. Cell Biol.* **74**:561–577.
24. FRÜHLING, J., W. PENASSE, G. SAND, and A. CLAUDE. 1969. Préservation du cholesterol dans la corticosurrenale rat au cors de la préparation des

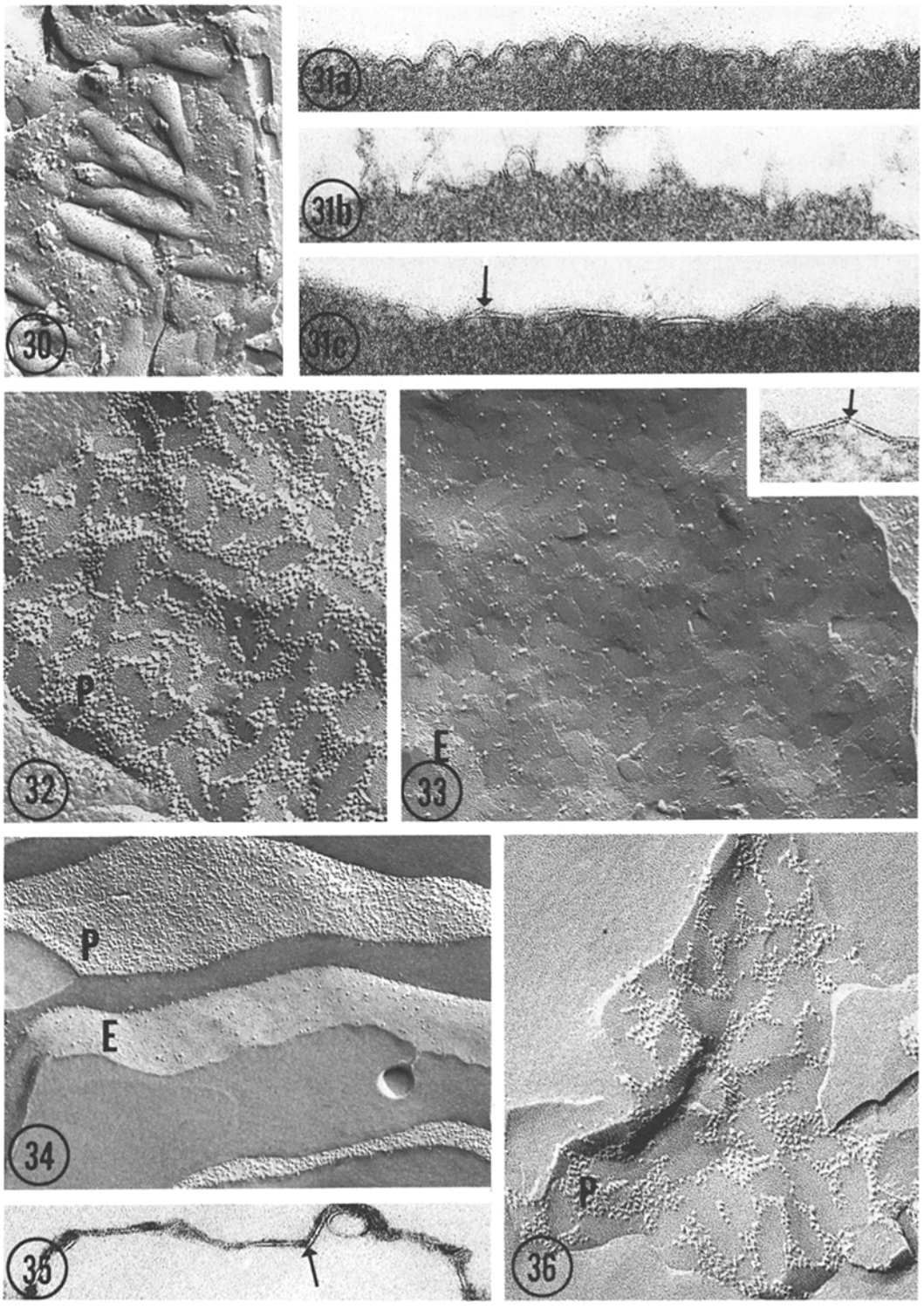
30
31a
31b
31c
32
P
33
E
34
P
E
35
36
P

tissues pour la microscopie eléctronique. *J. Microsc. Paris.* **9**:957–982.
25. FRÜHLING, J., W. PENNASE, W. SAND, E. MRENA, and A. CLAUDE. 1970. Étude comparative par microscopie eléctronique des reactions cytochemiques de la digitonine avec la cholesterol et d'autres lipides present dans les cellules de la corticosurrenale. *Arch. Int. Physiol. Biochim.* **78**:997–998.
26. GOODENOUGH, D. A., and W. STOECKENIUS. 1972. The isolation of mouse hepatocyte gap junctions. *J. Cell Biol.* **54**:646–656.
27. GRAHAM, R. C., JR., M. J. KARNOVSKY, A. W. SHAFER, E. A. GLASS, and M. L. KARNOVSKY. 1967. Metabolic and morphological observations on the effect of surface-active agents on leukocytes. *J. Cell Biol.* **32**:629–647.
28. HAEST, C. W. M., A. J. VERKLEIJ, J. DEGIER, R. SCHEEK, P. H. J. VERVERGAERT, and L. L. M. VAN DEENEN. 1974. The effect of lipid phase transitions on the architecture of bacterial membranes. *Biochim. Biophys. Acta.* **356**:17–26.
29. HENNING, R., H. D. KAULEN, and W. STOFFEL. 1973. Isolation and chemical composition of the lysosomal and the plasma membrane of the rat liver cell. *Hoppe-Seyler's Z. Physiol. Chem.* **351**:1191–1199.
30. HUANG, C. 1977. A structural model for the cholesterol-phosphatidylcholine complex in bilayer membranes. *Lipids.* **12**:348–356.
31. JAIN, M. H. 1975. Role of cholesterol in biomembranes and related systems. *Curr. Top. Membr. Res.* **6**:1–57.
32. JULIANO, R. L. 1973. The proteins of the erythrocyte membrane. *Biochim. Biophys. Acta.* **300**:341–378.
33. KASPER, C. B. 1974. Isolation and properties of the nuclear envelope. *Methods Enzymol.* **31**(A):279–292.
34. LANGE, V., and J. S. D'ALESSANDRO. 1977. Characterization of mechanisms for transfer of cholesterol between human erythrocytes and plasma. *Biochemistry.* **16**:4339–4343.
35. LEON, L., R. L. RUSH, and J. TURRELL. 1970. Automated simultaneous cholesterol and triglycerides determination on the Autoanalyzer II instrument. *In* Advances in Automated Analysis, Technician International Congress. Mediad Inc., White Plains, N. Y. **1**:503–507.
36. LEVY, M., R. TOURY, and J. ANDRÉ. 1967. Séparation des membranes mitochondrial. Purification et caractérisation enzymatique de la membrane externe. *Biochim. Biophys. Acta.* **135**:599–613.
37. MELCHIOR, D. L., and J. M. STEIN. 1976. Thermotropic transitions in biomembranes. *Annu. Rev. Biophys. Bioeng.* **5**:205–238.
38. MILLER, R. G. 1977. Crystalline patterns of myelin lipids visualized by freeze-fracture. *Biochim. Biophys. Acta.* **466**:325–335.
39. MOSES, J. L., W. W. DAVIS, A. J. ROSENTHAL, and L. D. GARREN. 1969. Adrenal cholesterol: localization by electron microscopic autoradiography. *Science (Wash. D. C.).* **163**:1203–1205.
40. NAPOLITANO, L. M., L. SALAND, J. LOPEZ, P. R. STERZING, and R. O. Kelley. 1972. Localization of cholesterol in peripheral nerve: Use of H^3 digitonin for electron microscopic autoradiography. *Anat. Rec.* **174**:157–164.
41. NICOLSON, G. 1976. Transmembrane control over the receptors on normal and tumor cells. I. Cytoplasmic influence over cell surface components. *Biochim. Biophys. Acta.* **457**:57–108.
42. ÖKROS, I. 1968. Digitonin reaction in electron microscopy. *Histochemie.* **13**:91–96.
43. PAPAHADJOPOULOS, D., M. COWDEN, and H. KIMELBERG. 1973. Role of cholesterol in membranes: effects on phospholipid-protein interactions, membrane permeability and enzymatic activity. *Biochim.*

FIGURES 30–33 Digitonin-treated whole human erythrocytes. Erythrocyte plasma membranes are quickly attacked by digitonin. Tubular complexes are only transiently visualized within membranes (Fig. 31*a*), and are quickly pulled into extracellular locales (Figs. 30 and 31*b*) as the cell progressively lyses. This process is unaffected by simultaneous fixation or pre-fixation with glutaraldehyde. More exhaustively treated specimens reveal extensive particle clustering on P fracture-faces (Fig. 32). Both P and E fracture-faces exhibit extensive membrane buckling into polygonal plates after corrugations are completely removed (Figs. 31*c*, 32, and 33). Fig. 30, × 72,500; Fig. 31*a–c*, × 80,000; Fig. 32, × 80,000; Fig. 33, × 54,000; insert, × 120,000.

FIGURES 34–36 Control and digitonin-treated human erythrocyte ghosts. Note that the ghosting methods employed in this study do not produce clustering (Fig. 34). The pattern of particle clustering and membrane buckling after digitonin treatment is identical to that observed in whole erythrocytes (Fig. 36; cf. Figs. 33*c*, 34, and 35). However, in contrast to whole erythrocytes, intramembrane corrugation (cf. Figs. 31, 32*a*, and 32*b*) is not encountered in early stages. Fig. 34, × 42,500; Fig. 35, × 93,750; Fig. 36, × 77,000.

Biophys. Acta. **330:**8-26.

44. PEARSE, B. M. F. 1976. Clathrin: A unique protein associated with intracellular transfer of membrane by coated vesicles. *Proc. Natl. Acad. Sci. U. S. A.* **73:**1255-1259.
45. PINTO DA SILVA, P. 1972. Translational mobility of the membrane intercalated particles of human erythrocyte ghosts. *J. Cell Biol.* **53:**777-787.
46. SALAND, L. C., and L. M. NAPOLITANO. 1977. Stabilization of cholesterol in myelin with digitonin: observation with polarized light. *J. Histochem. Cytochem.* **25:**280-286.
47. SCALLEN, T. J., and S. E. DIETERT. 1969. The quantitative retention of cholesterol in mouse liver prepared for electron microscopy by fixation in a digitonin-containing aldehyde solution. *J. Cell Biol.* **40:**802-813.
48. SINGER, S. J., and G. L. NICOLSON. 1972. The fluid mosaic model of the structure of cell membranes. *Science (Wash. D. C.).* **175:**720-731.
49. SIPERSTEIN, M. D. 1965. Comparison of the feedback control of cholesterol metabolism in liver and hepatoma. *In* Developmental and Metabolic Control Mechanisms and Neoplasia. The Williams & Wilkins Co., Baltimore. 427-451.
50. SPERRY, W. M. 1963. Quantitative isolation of sterols. *J. Lipid Res.* **4:**221-225.
51. SPETH, V., and F. WUNDERLICH. 1973. Membranes of *Tetrahymena*. II. Direct visualization of reversible transitions in biomembrane structure induced by temperature. *Biochim. Biophys. Acta.* **29:**621-628.
52. STECK, T. L. 1974. The organization of proteins in the human red blood cell membrane. *J. Cell Biol.* **62:**1-19.
53. STERZING, P. R., and L.M. NAPOLITANO. 1972. Tissue cholesterol preservation: factors associated with retention of cholesterol in rat sciatic nerve fixed for electron microscopy. *Anat. Rec.* **173:**485-492.
54. THINES-SEMPOUX, D. 1973. A comparison between the lysosomal and the plasma membrane. *Front. Biol.* **29:**278-299.
55. TURNER, J. D., and G. ROUSER. 1974. Removal of lipid from intact erythrocytes and ghosts by aqueous solutions and its relevance to membrane structure. *Lipids.* **9:**49-54.
56. VERVERGAERT, P. H. J. T., A. J. VERKLEIJ, J. J. VERHOEVEN, and P. F. ELBERS. 1973. Spray freezing of liposomes. *Biochim. Biophys. Acta.* **311:**651-654.
57. WARREN, G. B., M. D. HONSLEY, J. C. METCALF, and N. J. M. BIRDSALL. 1975. Cholesterol is excluded from the phospholipid annulus surrounding an active calcium transport protein. *Nature (Lond.).* **255:**684-687.
58. WEINSTEIN, R. S., J. K. KHODADAD, and T. L. STECK. 1978. Ultrastructural characterization of proteins at the natural surfaces of the red cell membrane. *In* Proceedings of the 4th International Conference on Red Cell Metabolism and Function. Ann Arbor, Mich. In press.
59. WILLIAMSON, J. R. 1969. Ultrastructural localization and distribution of free cholesterol (3-β-hydroxysterols) in tissues. *J. Ultrastruct. Res.* **27:**118-133.
60. WINDAUS, A. 1910. Über die Quantitative Bestimmung des Cholesterins und der Cholesterin-ester in Einigen normalen und pathologischen Nieren. *Hoppe-Seyler's Z. Physiol. Chem.* **65:**110-147.
61. WUNDERLICH, F., D. F. H. WALLACH, V. SPETH, and H. FISCHER. 1974. Differential effects of temperature on the nuclear and plasma membranes of lymphoid cells. *Biochim. Biophys. Acta.* **373:**34-43.